

---

The Journal of Nuclear Medicine

---

# JNMM

---

Volume 34, Number 9 • September 1993

---

---

1397 Role of  $^{123}\text{I}$ -Tyr-3-Octreotide Scintigraphy

---

1403 Scintimetric Evaluation of Remodeling

---

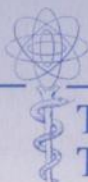
1410 Bone SPECT in Physeal Arrest

---

1577 Transmission CT for SPECT Attenuation Compensation

---

*Full Table of Contents Begins on Page 4A, Annotations on Pages 7A-8A*



---

The Official Publication of  
The Society of Nuclear Medicine, Inc.

---

**The Role of Iodine-123-Tyr-3-Octreotide Scintigraphy in the Staging of Small-Cell Lung Cancer**

Twenty patients with histologically confirmed SCLC and fifty radiologically staged tumor sites were investigated by an imaging protocol which included dynamic, static and SPECT studies ..... page 1397

**Scintimetric Evaluation of Remodeling After Bone Fractures in Man**

A retrospective screening of over 2000 patients who had undergone bone scintigraphy after trauma..... page 1403

**Diagnosis of Partial and Total Physical Arrest by Bone Single Photon Emission Computed Tomography**

The capability, limits and pitfalls of bone SPECT in the diagnosis of various types of epiphyseal development was evaluated by 75 bone SPECT studies in 64 children suspected of arrested growth development ..... page 1410

**Quantitative Analysis of the Technetium-99m-DTPA Captopril Renogram: Contribution of Washout Parameters to the Diagnosis of Renal Artery Stenosis**

Quantitative criteria used to diagnose renal artery stenosis was refined by retrospective analysis of pre- and postcaptopril DTPA renograms from 88 hypertensive patients, 45 of whom had RAS and 43 with normal renal arteries and angiography..... page 1416

**Initial Assessment of Positron Emission Tomography Using Fluorine-18-Fluoro-2-Deoxy-D-Glucose (FDG) in the Imaging of Malignant Melanoma**

PET studies of 12 patients imaged one hour after injection of 10 mCi of FDG were compared to physical examination, additional imaging studies and biopsy results. .... page 1420

**Technetium-99m-HMPAO Labeled Leukocytes and Technetium-99m-Labeled Human Polyclonal Immunoglobulin G (HIG) in the Diagnosis of Focal Purulent Disease**

Thirty-one comparative scintigraphies were performed in 30 patients with known or strongly suspected focal infection. Nineteen patients had focal

purulent disease as the final diagnosis. .... page 1428

**Lymphoscintigraphy in High-Risk Melanoma of the Trunk: Predicting Draining Node Groups, Defining Lymphatic Channels and Locating the Sentinel Node**

In 209 patients with high risk melanoma of the trunk, considered likely candidates for lymph node dissection, lymphoscintigraphy accurately defined draining lymph node groups and was 94% sensitive for detection of draining sites containing metastases. .... page 1435

**Evaluation of the Pulmonary Systemic Blood Flow Using ECG Gated Acquisition**

Based upon a proven relationship between periodic variations in local activity of labeled blood and pulsatile flow, the authors offer a method for the evaluation of systemic-to-pulmonary flows..... page 1441

**SPECT in Patients with Cortical Visual Loss**

SPECT with <sup>99m</sup>Tc-HMPAO was used to investigate changes in cerebral blood flow in seven patients with cortical visual impairment ..... page 1447

**Regional Cerebral Blood Flow-SPECT in Chronic Alcoholism: Relation to Neuropsychological Testing**

The central nervous systems of 40 asymptomatic chronic alcoholics and 20 age-matched controls were evaluated by neuropsychological testing, brain <sup>99m</sup>Tc-HMPAO SPECT and morphometric analysis by CT .... page 1452

**Comparability of FDG-PET Studies in Probable Alzheimer's Disease**

Patients with probable Alzheimer's disease were studied by FDG-PET in three different European centers utilizing different PET scanners to determine whether a single-study protocol could yield comparable results ..... page 1460

**Impact of Antianginal Medications, Peak Heart Rate and Level of Stress on the Prognostic Value of Normal Exercise Myocardial Imaging Perfusion Study**

Patients with a normal exercise <sup>201</sup>Tl study were followed for approximately two years to determine whether antianginal medications or the level of achieved stress affect the prognostic value of a normal exercise <sup>201</sup>Tl study. .... page 1467

**Nitrates Improve the Detection of Ischemic but Viable Myocardium by Thallium-201 ReInjection SPECT**

Twenty patients, 17 with a recent infarction, received nitrates postexercise to improve blood flow during the redistribution period and, potentially, to improve the sensitivity of reinjection imaging..... page 1472

**Myocardial Perfusion Imaging and Application of Graphical Analysis with Technetium-99m Tetrofosmin**

Using exercise-rest protocol, the <sup>99m</sup>Tc-tetrofosmin SPECT findings of 130 myocardial segments were classified as infarction, ischemia and partial filling and compared with those with <sup>201</sup>Tl. .... page 1478

**Rapid Back to Back Adenosine Stress/Rest Technetium-99m Teboroxime Myocardial Perfusion SPECT Using a Triple-Detector Camera**

Imaging parameters were determined and then applied in SPECT studies of 51 catheterized patients and 20 patients with a low likelihood of coronary artery disease..... page 1485

**Quantitative Same Day Rest-Stress Technetium-99m Sestamibi SPECT Definition and Validation of Normal Limits and Criteria for Abnormality**

Gender-matched stress normal limits and criteria for abnormality for rest-stress <sup>99m</sup>Tc sestamibi, same-day myocardial perfusion imaging were developed and validated in 160 patients. .... page 1494

**Detection of Doxorubicin Cardiotoxicity in Patients with Sarcomas by Indium-111-Antimyosin Monoclonal**

## Antibody Studies

Thirty patients with sarcomas who received radiotherapy were studied to assess myocardial cell damage due to doxorubicin cardiotoxicity ... *page 1503*

**Editorial: Antimyosin Positivity in Doxorubicin Cardiotoxicity: Earlier Than the Conventional Evidence** ..... *page 1507*

**Teboroxime, Sestamibi and Thallium-201 as Markers of Myocardial Hypoperfusion: Comparison by Quantitative Dual Isotope Autoradiography in Rabbits**  
The differential uptake of several imaging agents were compared in normal and hypoperfused rabbit myocardium. Rabbits with acute occlusions received dual or single isotope injections. A group of sham controls received teboroxime and/or <sup>201</sup>Tl..... *page 1510*

**Editorial: Measurement of Myocardial Blood Flow by Radiolabeled Tracers**..... *page 1518*

**Load Independence of Early Diastolic Filling Parameters in the Anesthetized Canine Model**  
Eleven atrially paced dogs underwent simultaneous micromanometer left atrial and left ventricular pressure measurements ..... *page 1520*

**Myocardial Substrate Utilization and Left Ventricular Function in Adriamycin Cardiomyopathy**  
Groups of rats were treated with adriamycin once a week for 6, 8, 9 and 10 weeks. Fluorine-18-FDG and <sup>125</sup>I-BMIPP were used as tracers of glucose and fatty acid metabolism, and <sup>99m</sup>Tc-MIBI as a myocardial blood flow tracer. Left ventricular ejection fraction calculated from gated blood pool images was used as an indicator of cardiac function ..... *page 1529*

**Chemistry and Biological Behavior of Samarium-153 and Rhenium-186-Labeled Hydroxylapatite Particles: Potential Radiopharmaceuticals for Radiation Synovectomy**  
The safety of <sup>153</sup>Sm and <sup>186</sup>Re-labeled hydroxylapatite particles was evaluated in normal rabbits and rabbits with anti-

gen-induced arthritis..... *page 1536*

**Phosphoinositide Turnover Imaging Linked to Muscarinic Cholinergic Receptor in Central Nervous System by Positron Emission Tomography**  
By means of in vivo autoradiography and PET, the authors attempted to visualize the phosphoinositide response to mAChR-stimulation in rats and monkeys ..... *page 1543*

**A Distributed Pharmacokinetic Model of Two-Step Imaging and Treatment Protocols: Application to Streptavidin-Conjugated Monoclonal Antibodies and Radiolabeled Biotin**  
The distribution of streptavidinylated antibody and radiolabeled biotin within a tumor was examined, and the two-step protocol compared with a one-step protocol using radiolabeled antibody. .... *page 1552*

**SIMS Microscopy Imaging of the Intratumor Biodistribution of Metaiodobenzylguanidine in Human SK-N-SH Neuroblastoma Cell Line Xenografted into Nude Mice**  
Highly specific images of MIBG biodistribution were mapped within the tumor after in vivo administration of the drug and sample processing with cryotechniques to prevent MIBG diffusion from original sites of uptake ..... *page 1565*

**Lung Tumor Metastasis to Breast Detected by Fluorine-18-Fluorodeoxyglucose PET**  
In a seven-week interval of PET studies monitoring the response of the primary lesion to radiation therapy, an area of markedly increased uptake of FDG appeared in the right breast. ... *page 1571*

**Paradoxical Changes in Iodine-131 Scintigraphic Findings in Advanced Follicular Thyroid Cancer**  
Lesions initially seen on <sup>131</sup>I scintigraphy but subsequently not visualized with scanning doses of <sup>131</sup>I retained their ability to produce increasing amounts of thyroglobulin and take up <sup>201</sup>Tl..... *page 1574*

**Fast Transmission Computed Tomography for Determining Attenuation Maps Using a Collimated, Shuttered Line Source Rotatable Air-Copper-Lead Attenuator and Fan-Beam Collimation**  
A method utilizing a line source and rotating air-copper-lead assembly to acquire gamma transmission computed tomographic data in order to determine attenuation maps and compensate SPECT emission scans. .... *page 1577*

**Brain Phantom Study: Accuracy of Registration of PET, SPECT and MR Images**  
The accuracy of a surface-fitting algorithm for three-dimensional image registration of SPECT, PET and MR images was tested using a three-dimensional water-fillable brain phantom. .... *page 1587*

**Three-Dimensional Dosimetry for Radioimmunotherapy Treatment Planning**  
A method for integrating functional data from SPECT or PET with anatomical data from CT or MRI is described. .... *page 1595*

**Left Ventricular Systolic and Diastolic Function Measurements Using an Ambulatory Radionuclide Monitor: Effects of Different Time Averaging on Accuracy**  
Fifty-one patients, comprising 67 studies, underwent equilibrium radionuclide angiography immediately before a Vest study. Agreement between Vest and RNA in estimating ejection fraction and peak filling rates was evaluated by computing the 'limits of agreement' ..... *page 1602*

**A Scintigraphic Sign for Detection of Right to Left Shunts**  
The usefulness of a new scintigraphic sign for the diagnosis of right-to-left shunt using <sup>99m</sup>Tc-MAA particles was evaluated by retrospective analysis of 49 <sup>99m</sup>Tc-MAA scintigrams ... *page 1607*

**Uptake of Tc-99m MDP in Primary Amyloidosis with a Review of the Mechanisms of Soft Tissue Localization of Bone-Seeking Radiopharmaceuticals**..... *page 1612*